



## Effect of Dual Releasing of $\beta$ -glycerophosphate and Dexamethasone from Ti Nanostructured Surface for Using in Orthopedic Applications

N. Hassanzadeh Nemati<sup>\*a</sup>, E. Ghasempour<sup>a</sup>, A. Zamanian<sup>b</sup>

<sup>a</sup> Department of Biomedical Engineering, Science and Research Branch, Islamic Azad University, Tehran, Iran

<sup>b</sup> Department of Nanotechnology and Advanced Materials, Materials and Energy Research Center (MERC), Karaj, Iran

### PAPER INFO

#### Paper History:

Received 13 February 2019

Received in revised form 11 September 2019

Accepted 12 September 2019

#### Keywords:

Anodizing

TiO<sub>2</sub> Nanotubes

Dual Releasing

Bone Replacements

$\beta$ -glycerophosphate

### ABSTRACT

Nano-structured surface and its ability to dual release of osteogenic and anti-inflammatory agents have a positive effect on the success of using titanium in orthopedic applications. For this purpose, TiO<sub>2</sub> nanotubes (TNTs) were created via anodization method on Ti sheets and loaded by  $\beta$ -glycerophosphate (GP) and dexamethasone (DEX) as osteogenic and anti-inflammatory agents, respectively. They were coated with a polyvinyl alcohol (PVA) layer for controlling their releasing rate. The synthesized dual-release system was characterized by field emission scanning electron microscopy (FE-SEM), Fourier transform infrared spectroscopy (FTIR) analysis, XRD and UV-Vis techniques. The average diameter of TNTs was 84.182 nm. The presence of drugs in the system has been proven in the FTIR analysis. UV-Vis technique's results show that the coated layer could control the release rate to improve the potential of the structures for supporting mineralization. Releasing of DEX was higher than GP and reached to a constant rate after 9 days. MTT test results confirmed the possibility of the surface designed Ti for bone regeneration purposes.

doi: 10.5829/ije.2019.32.10a.01

## 1. INTRODUCTION

Each drug has a specific therapeutic window. A higher or lower concentration leads to some side-effects or ineffectiveness [1]. In recent years, many researchers have paid attention to suitable drug delivery vehicles for their ability to transferring enough pharmaceutical agents especially to the target [2, 3]. Local releasing and minimizing drug intaking are the other advantages of the new drug delivery systems, especially in cancer therapy [4]. The problems of rapid degradation of drugs in the physiological environments before effectiveness could be also solved through engineered vehicles [5].

Nanotubes are examples of such efforts that could transfer therapeutic agents into cells [6].

There are various methods for TiO<sub>2</sub> nanotubes (TNTs) synthesis on Ti-based metals such as hydrothermal methods [7], Electrophoretic Synthesis [8] and electrochemical anode oxidation (anodization) [9].

Recently, high purity titanium is used as the basis for the growth of TiO<sub>2</sub> nanotube layers in an electrolyte containing fluoride ion. An array of the TNTs are formed after applying the appropriate potential for a specific period. The nanotube growth is based on the formation of the cavity in the interfacial of titanium sheet and created TiO<sub>2</sub> at the surface [10]. The ability of formation nanotubes on Ti and its alloys also makes them as biomaterials with an opportunity to act as biological agents delivery vehicles especially in bone regeneration applications [11].

Synthesis of TNTs has recently attracted great attention due to its excellent physical geometry, high surface area, unique electron and optical properties, high corrosion resistance, high thermal stability, antimicrobial properties, biocompatibility, non-toxicity and bioactivity [10]. These properties and the high surface to volume ratio make this material suitable for a wide range of biomedical applications [11-13], for example as

\*Corresponding Author Email: [hasanzadeh@srbiau.ac.ir](mailto:hasanzadeh@srbiau.ac.ir) (N. Hassanzadeh Nemati)

antimicrobial agents [14] and drug release systems [15]. In orthopedic applications, the possibility of optimal bone growth, cell differentiation, and the ability to form apatite layer on TiO<sub>2</sub> implants surfaces have been proven [16]. Studies have shown that the tubular structure of TiO<sub>2</sub> can be functionalized by bone growth factors that play a vital role in bone implantation [17]. It has also been shown that cell adhesion and the ability to regenerate bone can be increased by TiO<sub>2</sub> due to its high specific surface area [10]. Recent advances in stem cell research have shown that TiO<sub>2</sub> has the capability of differentiating mesenchymal stem cells into bone cells [18].

TNTs are widely used in drug-loaded implants in bone regeneration [19]. Shidfar et al. [20] synthesized TiO<sub>2</sub> nanotube arrays with a length to the diameter of 85:1 for delivery of gentamicin antibiotic in the implantation zone to a reduction of bacterial adhesions. They controlled the release rate by coating chitosan on the surface of nanotubes .

DEX is one of the corticosteroids which suppress the immune system and has anti-inflammatory and anti-sensitive effects [21]. DEX commonly used in allergy [22], inflammation [23] or arthritis [24] and respiratory infections [25]. Khodaverdi and et al. [26] loaded it in poly lactic-co-glycolic acid/polyethylene glycol hydrogels. Their results indicated the anti-inflammatory performance of structures and induction of cell differentiation.

GP is an organic phosphate compound, which is a material containing phosphate ions with ability of inducing MC3T3-E1 (mouse osteoblastic cells) differentiation [27]. Hamlin et al. [28] demonstrated that approximately 80 % of the GP has been hydrolyzed via bone cells within 24 hours, leading to the production of phosphate ions. Besides, GP increases the expression of the matrix protein gene, bone regeneration, matrix production and mineralization [29].

Polyvinylalcohol (PVA) is a synthetic, water-soluble and biocompatible polymer derived from polyvinyl acetate during the partial or total hydroxylation process [30]. Coating of PVA on drug delivery vehicles can control the releasing rate of drugs [31].

The creation of a system containing titanium nanotubes with a polymer coat with dual releasing of DEX and GP capability is one of the research innovations. For this purpose, titanium sheets were modified via the anodizing method and then GP was loaded into the synthesized TNTs. At the second step, the surface of TNTs were coated with the DEX loaded PVA to reduce GP release rate. The samples were characterized by SEM, FTIR, EDX spectrum, XRD peaks, and UV-Vis analysis. Finally, for assessing biocompatibility, MTT assay was carried out.

## 2. MATERIALS AND METHODS

### 2. 1. Synthesis of TNTs by Anodizing Method

Titanium sheets (99.7% purity, Aldrich-Sigma Co) with the dimensions of 15×10×1.5 mm<sup>3</sup> were mechanically polished to reach the mirror and smooth surface. Then, they were washed with ethanol and deionized water and dried under atmospheric air. In the anodizing process, the titanium sheet and the 30×30 mm<sup>2</sup> platinum mesh were used as anode and cathode, respectively. The solution including HF (1% v/v) and 3wt.% deionized water in ethylene glycol (anhydrous, 99.8%purity, Sigma–Aldrich Co) was used as the electrolyte. The process was performed at ambient temperature for 20 minutes (voltage of 23 V). The distance between anode and cathode was 2cm. Finally, the samples were washed with ethanol and deionized water and dried under nitrogen gas.

**2. 2. Loading GP in TNTs** The anodized Ti sheets were immersed in β-glycerophosphate (GP, Mw 216.04 g/mol, Merck, Germany) with a concentration of 1.53 mg/ml for 30 minutes under vacuum. Then, the samples were dried for 15-20 minutes (ambient temperature, vacuum). Drug loading and drying procedures were repeated five times for adequate loading of GP .

### 2. 3. coating DEX-loaded PVA on the Surface on TNTs

The PVA (Mw 200000 kDa, d: 1.3 g/cm<sup>3</sup>, Merck Co) solution at a concentration of 1% w/v was prepared at 150 °C and was stirred 24 hours at 1200 rpm. Then, DEX (Mw 472.44 g/mol, Merck Co) with a concentration of 1.96 mg/ml was added to the homogeneous PVA solution. Subsequently, GP loaded TNTs (TNT-GP) were immersed in the prepared solution with the rate of 10 mm/min for 4 hours. The immersion process was repeated 10 times. Finally, the immersed specimens were dried at 30 °C for 15 minutes. The coated samples were cross-linked via the glutaraldehyde: HCl vapor (1:10 molar ratio) for 12 hours. The samples were immersed in SBF solution which had been prepared by conventional Kokubo method [32] and refreshed every 2 days for 7 and 14 days .

B-glycerophosphate loaded TiO<sub>2</sub> Nanotubes and PVA-Dexamethasone coating on B-glycerophosphate loaded TiO<sub>2</sub> Nanotubes were encoded TNT-GP and TNT-GD, respectively.

**2. 4. Characterization** The microstructure of the samples was studied at 15kv by FE-SEM (TESCAN MIRA3 LMU).

Attenuated total reflection Fourier Transform Infrared Spectroscopy (ATR-FTIR, Bruker Vector33, Germany) was used in the wavenumber of 400-4000 cm<sup>-1</sup>

wave number to ensure the chemical compositions of structure and formation of the coating layer Calibration curve of GP and DEX was obtained based on the following procedure. Therefore, stock solution (10 mg/ml) was prepared by solubilizing GP and DEX in an aqueous solvent. Then, five solutions with the concentrations of 5 mg/ml, 3.33, 2.5, 2, 1.33, 1 and 0.9 mg/ml were prepared by dilution of the solution. Absorption was measured at maximum wavelengths of 203.5 nm for GP and 242 nm for DEX.

Drug releasing behavior of the samples were determined by ultraviolet-visible spectroscopy (WPA biowave II, Biochrom company, Britain). This test was repeated 5 times to obtain the mean and standard deviation. For this purpose, TNT-GP and GP and DEX loaded TiO<sub>2</sub> (TNT-GD) samples were immersed in 5 ml of PBS solution and shaken by thermoshaker (LS100, Gerhardt company, USA) at 30 rpm and temperature of 37 °C.

Hydroxyapatite formation was proved by a phase analysis using an X-ray diffraction device (Philips PW3710 model) with monochromatic Cu-K $\alpha$  radiation (1.54178Å wavelength). The morphology of the deposited layer was investigated via FE-SEM images and elemental characterization of this layer followed by energy-dispersive X-ray diffraction spectrometry (EDS) (TESCAN MIRA3 LMU model).

For Cellular interactions studying, Cell suspensions of osteoblasts G-292 cell line (Pasteur Institute of Iran) were cultured in a 24 house polystyrene well plate (5% CO<sub>2</sub>, 37 °C). Cells were detached from well plate surface using 0.25% Trypsin/EDTA enzyme and were placed on a cell culture plate with  $1 \times 10^4$  cells in each well. The cell was incubated by RPMI 1640 media containing 10% FBS, 100 U/ml penicillin-streptomycin. The morphology of the samples were examined by SEM. Therefore, the cell culture medium was removed and implants were washed once with PBS for 10 minutes. Then, they were placed in 2.5% glutaraldehyde diluted in PBS for 1 hour and 15 minutes. The previous solution was removed and the sheets were washed once with 1 ml of PBS serum. Fixed constructs were dehydrated using an ascending concentration of ethanol, namely 50, 60, 70 and 80% ethanol for 5 minutes and 90% ethanol for 5 and 7 minutes.

To study the biocompatibility of TNT and TNT-GD samples, L-929 fibroblast cells were cultured in well-plate and kept in an incubator at 37 °C and 90% humidity for 24 hours (culture medium RPMI 140, containing 10% FBS and 1% antibiotic penicillin-streptomycin). Fibroblast cells were obtained from Pasteur Institute of Iran. Subsequently, the cells were cultured on the surface of the samples at 37 °C and 90% humidity for 48 hours. Then, the culture medium was replaced with 100  $\mu$ l of culture medium containing 10% of the 3-[4,5-dimethylthiazol-2-yl]-2,5-diphenyltetrazolium bromide

(MTT) solution and incubated in darkness at 37 °C. After 4 hours, the MTT medium was removed and 100  $\mu$ l of DMSO solution was added. After 20 minutes, the solvent was pipetted in each house and then measured by an ELISA reader (BioShare Biowave2) at a wavelength of 570 nm. Each experiment was repeated three times.

**2. 5. Statistical Analysis** Data were processed using Microsoft Excel 2013 software and the results were presented as the mean  $\pm$  one standard deviation of at least three experiments. Statistical analysis was performed by using one-way ANOVA and Tukey test with significance reported when  $P < 0.05$ .

### 3. RESULTS AND DISCUSSION

**3. 1. Morphology Observation** Surface morphology of the samples (Figure 1) was observed by FE-SEM images. Figure 1 (a) indicated Ti sheet surface after polishing. As shown in Figure 1 (b), after the anodizing process, a uniform TNTs was created with an approximate average diameter of  $84.182 \pm 2$  nm and a wall thickness of 13.505 nm at the surface of the titanium substrate. The dimensions of TNTs were measured by Image J software. Figure 1 (c) illustrates the SEM micrographs of the nanotubes after GP loading. Accumulation of GP in the opening route of nanotubes distort the nanotubes shape. Figure 1 (d) shows the DEX-loaded PVA coating on the surface of TNTs. Results demonstrated uniform and homogeneous coating with PVA.

**3. 2. Chemical Characterization** Figure 2 indicates FTIR spectra of the raw and prepared samples.

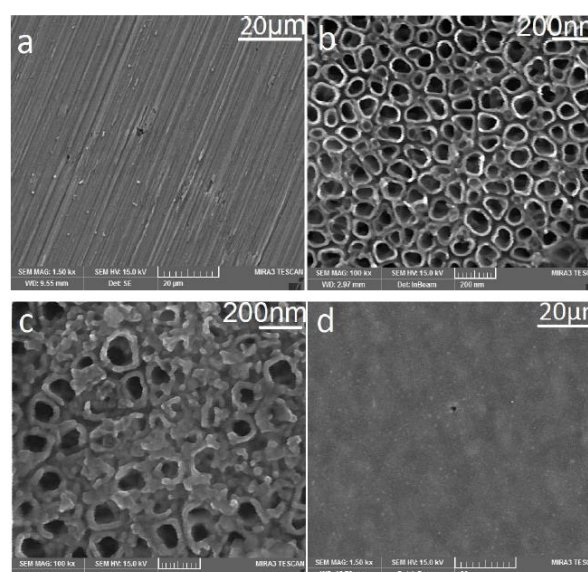


**Figure 1.** FE-SEM micrograph of pure Ti substrate (a) TNTs (b), TNT-GP (c) and TNT-GD (d)

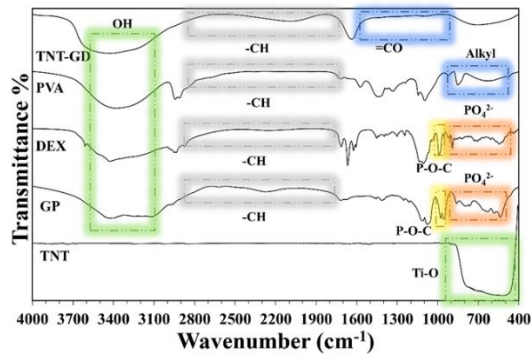


**Figure 2.** FTIR spectra of the TiO<sub>2</sub> nanotube (TNTs), GP, DEX, PVA, and TNT-GD

In all samples except TNTs, the broad peaks in the range of 3000-3500 cm<sup>-1</sup>, 1440-2900 cm<sup>-1</sup>, and 1200-1700 cm<sup>-1</sup> belong to stretching vibration of OH, CH and CO groups, respectively [33]. At the FTIR spectra of TNT

sample, the broad peak appears in the range of 400-850 cm<sup>-1</sup> which is attributed to the Ti-O vibrations [34]. In GP spectra, the peaks in the range of 530-786 cm<sup>-1</sup> and 1075 cm<sup>-1</sup> are related to PO<sub>4</sub><sup>3-</sup> group bonds. The two peaks in the ranges 978 cm<sup>-1</sup> and 1074 cm<sup>-1</sup> in DEX and GP correspond with the stretching vibration of P-O-C groups [35]. In pure PVA, the peak in the range of 500-900 cm<sup>-1</sup> is related to the main structure of the alkyl group presented in the polyvinyl alcohol structure [36]. The presence of broad and severe peaks in the mentioned range in the TNT-GD sample represents the overlapping of these peaks.

**3.3. Drug Release Behavior** The release behavior of GP and DEX were investigated using UV-VIS spectroscopy. Figure 3 (a, b) shows the standard curve for GP and DEX which were obtained at 203.5 and 242 nm in the concentration range of 0-10 mg/ml by UV-Vis spectrometry.

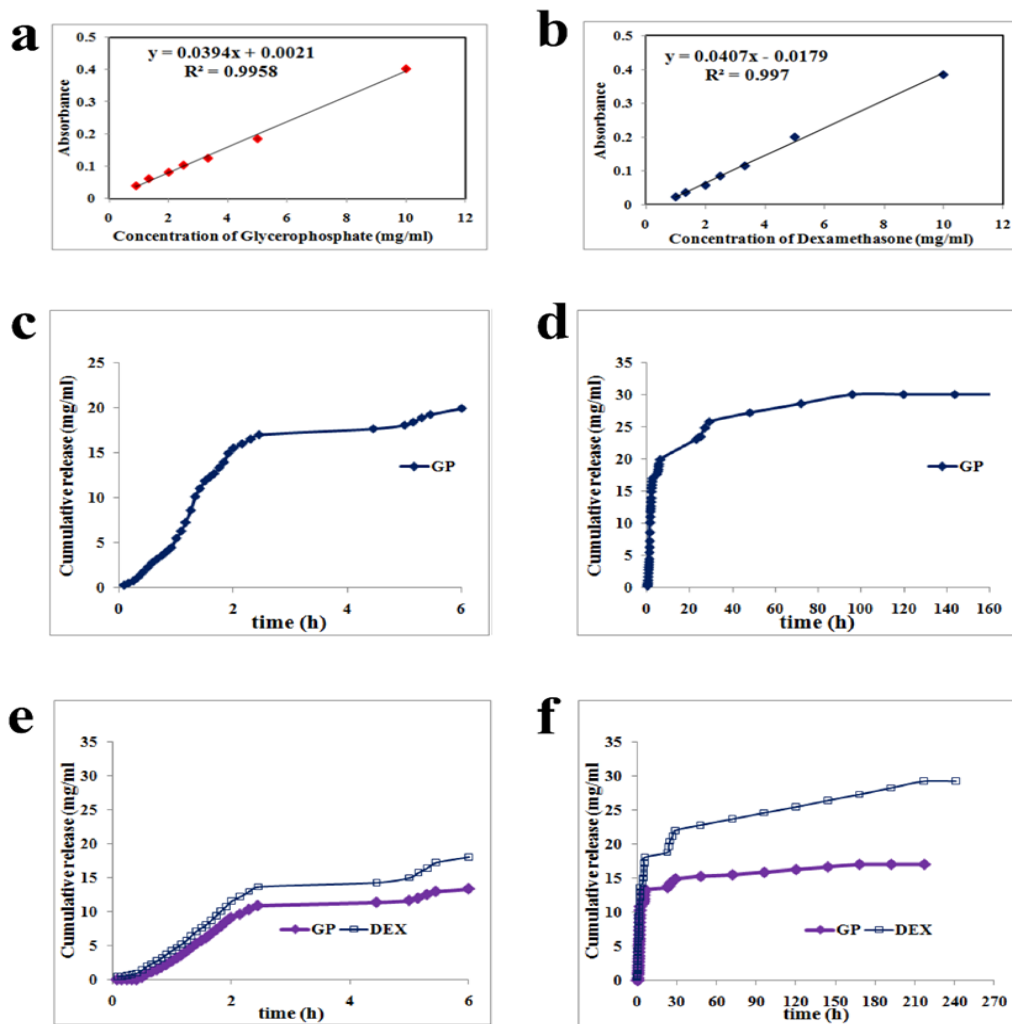


**Figure 3.** Calibration curve of GP (a) and DEX (b) at 203.5 and 242 nm. Release profile and accumulation release of TNT-GP and TNT-GD samples after 6 hours (c, e) and 10 days (d, f)

The accumulative single and dual release profiles from nanotubes after 6 hours and 10 days are shown in Figure 3 (c-f). The results demonstrated that the release profile in both samples had biphasic behavior, as Aw et al. [37] reported before. The first 2 hours consists of an initial sudden release. After that, the release rate follows a gradual and slow rate until reaches a constant value. In the case of TNT-GP, GP release showed a steep slope due to the high concentration of GP in the nanotubes and rapid release ratio. This ratio followed a steady gradient after 4 days. In a drug release system, the release behavior is as important as optimal drug loading to achieve a sustained and stable drug release profile during the time. The results showed that the rate and sudden releasing of both GP and DEX are reduced by applying PVA coatings on the surface of TNTs. In the gradual release zone, GP exhibited a slower release in the coated sample compared with the other ones. After 7 days, GP releasing reached a constant value higher than the TNT-GP sample. In the dual releasing system, releasing rate of GP was lower than DEX. This is because of GP blocking by PVA. Releasing of DEX reached a constant value after 9 days.

### 3. 4. Bioactivity

Figures 4 and 5 show SEM micrographs and EDS spectrum of the samples after 7 and 14 days immersion in SBF solution, respectively. The evidence demonstrated hydroxyapatite nucleation during 7 days in both test groups. However, the amount of hydroxyapatite was significant in TNT-GD one in which a thin layer of hydroxyapatite covered the surface (Figure 4 (a, c)). After 14 days immersion in the SBF solution, the density of the deposited hydroxyapatite increased but, still, there is an obvious difference between TNT and TNT-GD (Figure 5(a, c)). In addition, according to the EDS results on a 14-day soaking, the amount of mineralization increased in both TNTs and TNT-GD constructs, which is consistency with the FE-SEM images. The weight ratios of Ca/P were calculated to be 0.84 and 1.10 for TNTs sample after 7 and 14 days immersion in SBF, respectively. These ratios increased to 1.11 and 1.21 for TNT-GD samples after the same times, respectively. These results confirmed the increasing trend of hydroxyapatite formations on the loaded sample. It was due to the presence of phosphate ions in GP and DEX structures. These phosphate groups in GP and DEX contribute to the absorption of calcium and phosphorus from SBF solution due to their phosphate ions and increase the deposition of hydroxyapatite crystals [27, 29]. Therefore, the simultaneous use of GP and DEX act as phosphate ion supplier which significantly increases bioactivity.

The results of XRD analysis (Figure 6) confirmed the above-mentioned observations (comparing the analysis results with JCPDS Card No. 9-432). In TNT-GD

sample, the intensity of hydroxyapatite related peaks increased after the drug loading procedure. The intensity of apatite-related peaks also increased after 14 days of soaking. The results proved the ability of constructs to support bioactivity behavior.

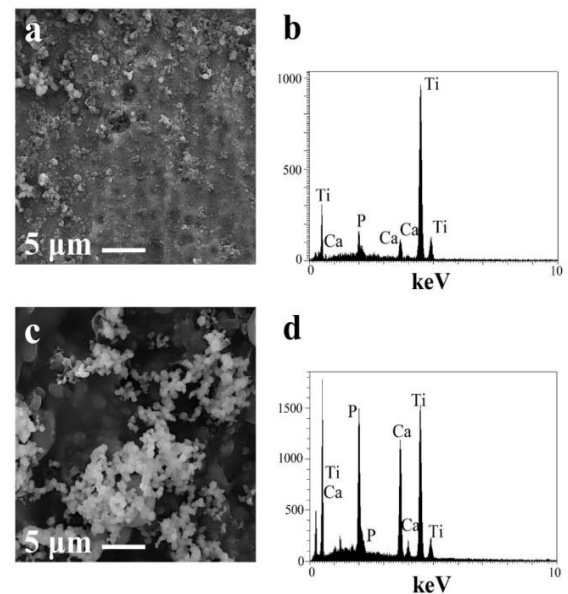


**Figure 4.** SEM morphology and EDS analysis of TNTs (a, b) and TNT-GD (c, d) after 7 days immersion in SBF solution

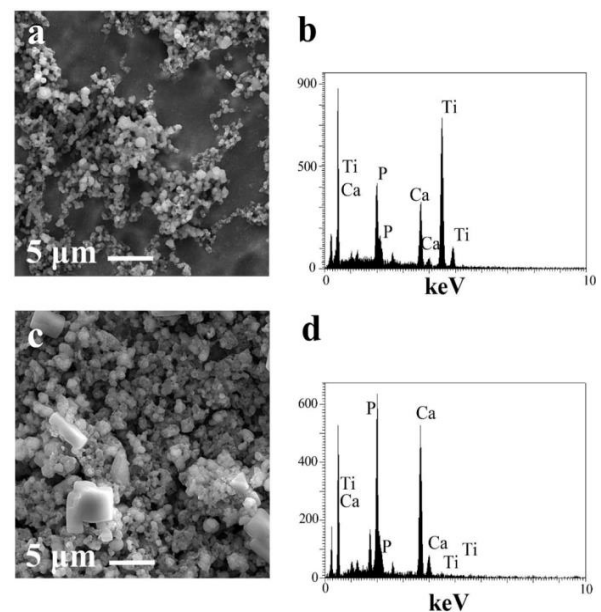


**Figure 5.** SEM morphology and EDS analysis of TNTs (a, b) and TNT-GD (c, d) after 14 days immersion in SBF solution

**3. 5. Cellular Interactions** Figure 7 (a, b) shows SEM micrographs of G-292 cells morphology on the TNTs and TNT-GD implants after 48 hours culturing time. The images indicate the presence of GP and DEX in TNT-GD improved cell adhesion. Fratzi-Zelman et al. [38] demonstrated that GP and DEX could be a source of phosphate ions as a result of hydrolysis via cells in physiologic media.

Biocompatibility of TNTs and TNT-GD specimens were evaluated by a 48-hour cytotoxicity test (Figure 7 (c)). The polystyrene cell culture plate with 100% viability was considered as a control group. The cellular viability of TNTs and TNT-GD substrate was achieved about 87.55% and 95.64%, respectively. The viability of more than 85% cells in comparison with control group proved the biocompatible performance of the specimen. Vacanti et al. [39] and Szymanska et al. [40] demonstrated before that DEX and GP exhibit good biocompatibility in controlled one agent releasing vehicles, respectively. At the present research, it is shown that the dual releasing system of GP and DEX contain PVA coating enhanced biological properties of the anodized Ti.

#### 4. CONCLUSION

In this study, the titanium surface was anodized in order to prepare uniform bioactive nanotubes with a capacity

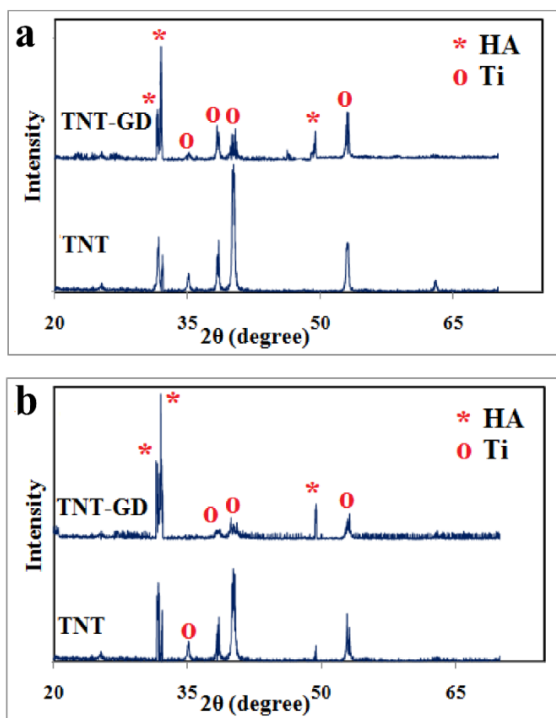


**Figure 6.** XRD analysis of TNTs and TNT-GD after 7 (a) and 14 (b) days immersion in SBF solution

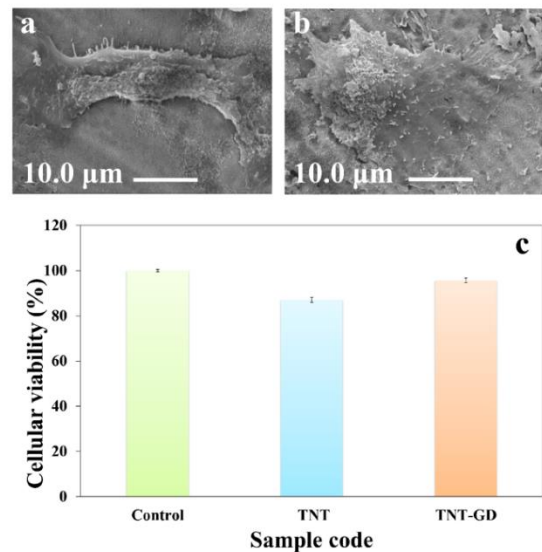


**Figure 7.** SEM micrographs of the osteoblasts G-292 cell line on TNTs (a) and TNT-GD (b). The cell viability of L929 fibroblasts seeded on TNTs and TNT-GD sample (c)

of drug loading. GP was loaded in TNTs as a bioactive factor to promote osteogenic behavior of implants. Coating the surface via PVA helped to control the release rate of GP. Besides, the DEX was loaded in PVA layer as an anti-inflammatory and bioactive factor. The result indicated that loading the GP and DEX and homogeneous coating the TNTs improve mineralization of samples and control the burst release of loaded factors. Moreover, the ability to modify implants to support cell adhesion and lack of any sign of toxicity that could make them good candidates for bone replacement applications.

#### 5. REFERENCES

- Jalali, N., Moztarzadeh, F., Mozafari, M., Asgari, S., Shokri, S. and Alhosseini, S.N., "Chitosan-surface modified poly (lactide-co-glycolide) nanoparticles as an effective drug delivery system", in 2011 18th Iranian Conference of Biomedical Engineering (ICBME), IEEE., (2011), 109-114.
- Demirdöğen, R.E., Emen, F.M., Ocakoglu, K., Murugan, P., Sudesh, K. and Avşar, G., "Green nanotechnology for synthesis and characterization of poly (3-hydroxybutyrate-co-3-hydroxyhexanoate) nanoparticles for sustained bortezomib release using supercritical CO<sub>2</sub> assisted particle formation combined with electrodeposition", *International Journal of Biological Macromolecules*, Vol. 107, (2018), 436-445.
- Liang, P.-C., Huang, K.-W., Tung, C.-C., Chang, M.-C., Chang, F.-Y., Wong, J.-M. and Chang, Y.-T., "A novel photodynamic therapy-based drug delivery system layered on a stent for treating cholangiocarcinoma", *Biomedical Microdevices*, Vol. 20, No. 1, (2018), DOI: 10.1007/s10544-017-0249-1.
- Tan, Y., Zhu, Y., Zhao, Y., Wen, L., Meng, T., Liu, X., Yang, X., Dai, S., Yuan, H. and Hu, F., "Mitochondrial alkaline pH-responsive drug release mediated by celastrol loaded glycolipid-

- like micelles for cancer therapy", *Biomaterials*, Vol. 154, (2018), 169-181.
5. Nicolas, J., Mura, S., Brambilla, D., Mackiewicz, N. and Couvreur, P., "Design, functionalization strategies and biomedical applications of targeted biodegradable/biocompatible polymer-based nanocarriers for drug delivery", *Chemical Society Reviews*, Vol. 42, No. 3, (2013), 1147-1235.
  6. Sadmezhaad, S. and Abbaspour, S., "Loading drug on nanostructured ti6al4v-ha for implant applications", *International Journal of Engineering-Transaction B: Applications*, Vol. 31, No. 8, (2018), 1159-1165.
  7. Liu, N., Chen, X., Zhang, J. and Schwank, J.W., "A review on tio2-based nanotubes synthesized via hydrothermal method: Formation mechanism, structure modification, and photocatalytic applications", *Catalysis Today*, Vol. 225, (2014), 34-51.
  8. Nourmohammadi, A., Mehrjueeb, M. and Bahrevarc, M., "Electrophoretic synthesis of titanium oxide nanotubes", *International Journal of Engineering-Transactions A: Basics*, Vol. 25, No. 4, (2012), 343-350.
  9. Wang, J., Li, H., Sun, Y., Bai, B., Zhang, Y. and Fan, Y., "Anodization of highly ordered TiO<sub>2</sub> nanotube arrays using orthogonal design and its wettability", *International Journal of Electrochemical Science*, Vol. 11, (2016), 710-723.
  10. Wilczewska, A.Z., Niemirowicz, K., Markiewicz, K.H. and Car, H., "Nanoparticles as drug delivery systems", *Pharmacological Reports*, Vol. 64, No. 5, (2012), 1020-1037.
  11. Wei, F., Li, M., Crawford, R., Zhou, Y. and Xiao, Y., "Exosome-integrated titanium oxide nanotubes for targeted bone regeneration", *Acta Biomaterialia*, Vol. 86, (2019), 480-492.
  12. Paulose, M., Peng, L., Popat, K.C., Varghese, O.K., LaTempa, T.J., Bao, N., Desai, T.A. and Grimes, C.A., "Fabrication of mechanically robust, large area, polycrystalline nanotubular/porous TiO<sub>2</sub> membranes", *Journal of Membrane Science*, Vol. 319, No. 1-2, (2008), 199-205.
  13. Prakasam, H.E., Shankar, K., Paulose, M., Varghese, O.K. and Grimes, C.A., "A new benchmark for TiO<sub>2</sub> nanotube array growth by anodization", *The Journal of Physical Chemistry C*, Vol. 111, No. 20, (2007), 7235-7241.
  14. Wen, J., Li, Q., Li, H., Chen, M., Hu, S. and Cheng, H., "Nano-TiO<sub>2</sub> imparts amidoximated wool fibers with good antibacterial activity and adsorption capacity for uranium (vi) recovery", *Industrial & Engineering Chemistry Research*, Vol. 57, No. 6, (2018), 1826-1833.
  15. Zhang, T., Xie, C., Liu, Y., Zhang, F. and Xiao, X., "Ph-responsive drug release system of Cu<sup>2+</sup>-modified ammoniated TiO<sub>2</sub> nanotube arrays", *Materials Letters*, Vol. 215, (2018), 95-98.
  16. Oh, S.-H., Finones, R.R., Daraio, C., Chen, L.-H. and Jin, S., "Growth of nano-scale hydroxyapatite using chemically treated titanium oxide nanotubes", *Biomaterials*, Vol. 26, No. 24, (2005), 4938-4943.
  17. Zhang, W., Zhang, Z. and Zhang, Y., "The application of carbon nanotubes in target drug delivery systems for cancer therapies", *Nanoscale Research Letters*, Vol. 6, No. 1, (2011), 555.
  18. von der Mark, K., Bauer, S., Park, J. and Schmuki, P., "Another look at "stem cell fate dictated solely by altered nanotube dimension""", *Proceedings of the National Academy of Sciences*, Vol. 106, No. 24, (2009), E60-E60.
  19. Johari, N., Hosseini, H.R.M. and Samadikuchaksaraei, A., "Novel fluoridated silk fibroin/ TiO<sub>2</sub> nanocomposite scaffolds for bone tissue engineering", *Materials Science and Engineering: C*, Vol. 82, (2018), 265-276.
  20. Shidfar, S., Tavangarian, F., Nemati, N.H. and Fahami, A., "Drug delivery behavior of titania nanotube arrays coated with chitosan polymer", *Materials Discovery*, Vol. 8, (2017), 9-17.
  21. Christensen, D.B. and Farris, K.B., "Pharmaceutical care in community pharmacies: Practice and research in the us", *Annals of Pharmacotherapy*, Vol. 40, No. 7-8, (2006), 1400-1406.
  22. Torkildsen, G., Abelson, M.B., Gomes, P.J., McLaurin, E., Potts, S.L. and Mah, F.S., "Vehicle-controlled, phase 2 clinical trial of a sustained-release dexamethasone intracanalicular insert in a chronic allergen challenge model", *Journal of Ocular Pharmacology and Therapeutics*, Vol. 33, No. 2, (2017), 79-90.
  23. Chaudhary, N., Arora, I., Gupta, D. and Gupta, C.P., "Comparison of efficacy and safety of dexamethasone 0.1% and difluprednate 0.05% in the management of ocular inflammation after phacoemulsification", *Journal of Evolution of Medical and Dental Sciences-Jemds*, Vol. 4, No. 74, (2015), 12899-12903.
  24. Wang, Q., Jiang, H., Li, Y., Chen, W., Li, H., Peng, K., Zhang, Z. and Sun, X., "Targeting nf-kb signaling with polymeric hybrid micelles that co-deliver sirna and dexamethasone for arthritis therapy", *Biomaterials*, Vol. 122, (2017), 10-22.
  25. Euba, B., Moleres, J., Segura, V., Viadas, C., Morey, P., Moranta, D., Leiva, J., de-Torres, J.P., Bengoechea, J.A. and Garmendia, J., "Genome expression profiling-based identification and administration efficacy of host-directed antimicrobial drugs against respiratory infection by nontypeable haemophilus influenzae", *Antimicrobial Agents and Chemotherapy*, Vol. 59, No. 12, (2015), 7581-7592.
  26. Khodaverdi, E., Kheirandish, F., Mirzazadeh Tekie, F.S., Khashyarmansh, B.Z., Hadizadeh, F. and Moallemzadeh Haghghi, H., "Preparation of a sustained release drug delivery system for dexamethasone by a thermosensitive, in situ forming hydrogel for use in differentiation of dental pulp", *ISRN Pharmaceutics*, Vol. 2013, (2013), DOI: 10.1155/2013/983053.
  27. Park, J.-B., "The effects of dexamethasone, ascorbic acid, and  $\beta$ -glycerophosphate on osteoblastic differentiation by regulating estrogen receptor and osteopontin expression", *Journal of Surgical Research*, Vol. 173, No. 1, (2012), 99-104.
  28. Hamlin, N. and Price, P., "Mineralization of decalcified bone occurs under cell culture conditions and requires bovine serum but not cells", *Calcified Tissue International*, Vol. 75, No. 3, (2004), 231-242.
  29. Boskey, A.L., Guidon, P., Doty, S.B., Stiner, D., Leboy, P. and Binderman, I., "The mechanism of  $\beta$ -glycerophosphate action in mineralizing chick limb-bud mesenchymal cell cultures", *Journal of Bone and Mineral Research*, Vol. 11, No. 11, (1996), 1694-1702.
  30. Kamoun, E.A., Kenawy, E.-R.S. and Chen, X., "A review on polymeric hydrogel membranes for wound dressing applications: Pva-based hydrogel dressings", *Journal of Advanced Research*, Vol. 8, No. 3, (2017), 217-233.
  31. Kayal, S. and Ramanujan, R., "Doxorubicin loaded pva coated iron oxide nanoparticles for targeted drug delivery", *Materials Science and Engineering: C*, Vol. 30, No. 3, (2010), 484-490.
  32. Ohtsuki, C., "How to prepare the simulated body fluid (SBF) and its related solutions, proposed by kokubo and his colleagues", Graduate school of materials science, Nara Institute of Science and Technology, (2009).
  33. Chen, L., Tang, C., Chen, D., Wong, C. and Tsui, C., "Fabrication and characterization of poly-dl-lactide/nano-hydroxyapatite composite scaffolds with poly (ethylene glycol) coating and dexamethasone releasing", *Composites Science and Technology*, Vol. 71, No. 16, (2011), 1842-1849.
  34. Kumar, P.M., Badrinarayanan, S. and Sastry, M., "Nanocrystalline TiO<sub>2</sub> studied by optical, ftr and x-ray photoelectron spectroscopy: Correlation to presence of surface states", *Thin Solid Films*, Vol. 358, No. 1-2, (2000), 122-130.
  35. Sahoo, P., Panda, H. and Bahadur, D., "Studies on the stability and kinetics of drug release of dexamethasone phosphate

- intercalated layered double hydroxides nanohybrids", *Materials Chemistry and Physics*, Vol. 142, No. 1, (2013), 106-112.
36. Mabrouk, M., Mostafa, A., Oudadesse, H., Mahmoud, A.A. and El-Gohary, M.I., "Effect of ciprofloxacin incorporation in pva and pva bioactive glass composite scaffolds", *Ceramics International*, Vol. 40, No. 3, (2014), 4833-4845.
  37. Aw, M.S., Gulati, K. and Losic, D., "Controlling drug release from titania nanotube arrays using polymer nanocarriers and biopolymer coating", *Journal of Biomaterials and Nanobiotechnology*, Vol. 2, No. 05, (2011), 477-484.
  38. Fratzl-Zelman, N., Fratzl, P., Hörandner, H., Grabner, B., Varga, F., Ellinger, A. and Klaushofer, K., "Matrix mineralization in mc3t3-e1 cell cultures initiated by  $\beta$ -glycerophosphate pulse", *Bone*, Vol. 23, No. 6, (1998), 511-520.
  39. Vacanti, N.M., Cheng, H., Hill, P.S., Guerreiro, J.o.D., Dang, T.T., Ma, M., Watson, S.e., Hwang, N.S., Langer, R. and Anderson, D.G., "Localized delivery of dexamethasone from electrospun fibers reduces the foreign body response", *Biomacromolecules*, Vol. 13, No. 10, (2012), 3031-3038.
  40. Szymańska, E., Sosnowska, K., Milyk, W., Rusak, M., Basa, A. and Winnicka, K., "The effect of  $\beta$ -glycerophosphate crosslinking on chitosan cytotoxicity and properties of hydrogels for vaginal application", *Polymers*, Vol. 7, No. 11, (2015), 2223-2244.

## Effect of Dual Releasing of $\beta$ -glycerophosphate and Dexamethasone from Ti Nanostructured Surface for Using in Orthopedic Applications

N. Hassanzadeh Nemati<sup>a</sup>, E. Ghasempour<sup>a</sup>, A. Zamanian<sup>b</sup>

<sup>a</sup> Department of Biomedical Engineering, Science and Research Branch, Islamic Azad University, Tehran, Iran

<sup>b</sup> Department of Nanotechnology and Advanced Materials, Materials and Energy Research Center (MERC), Karaj, Iran

### P A P E R I N F O

چکیده

#### Paper History:

Received 13 February 2019

Received in revised form 11 September 2019

Accepted 12 September 2019

#### Keywords:

Anodizing

TiO<sub>2</sub> Nanotubes

Dual Releasing

Bone Replacements

$\beta$ -glycerophosphate

سطح نانوساختار و توانایی آن در انتشار دوگانه‌ی عوامل استخوان‌ساز و ضد التهابی، تأثیر مثبتی در موفقیت استفاده از تیتانیوم در کاربردهای ارتوپدی دارد. برای این منظور، نانولوله‌های TiO<sub>2</sub> با استفاده از روش آندایزاسیون روی ورق‌های Ti ایجاد و به ترتیب توسط  $\beta$ -گلیسرופسفات (GP) و دگزامتازون (DEX) به عنوان عوامل استیوژنیک و ضدالتهابی بارگذاری شدند. برای کنترل میزان رهاسازی آنها، فویل‌های آندایز شده با یک لایه‌ی پلی وینیل الکل (PVA) پوشش داده شدند. سیستم انتشار دوگانه‌ی ساخته شده توسط میکروسکوپ الکترونی روبشی انتشار (FE-SEM)، طیف‌سنج مادون قرمز تبدیل (FTIR)، XRD و تکنیک‌های UV-Vis ارزیابی شد. متوسط قطر نانولوله‌ها ۸۴.۱۸۲ نانومتر بود. وجود داروها در سیستم در تحلیل FTIR ثابت شده است. نتایج تکنیک UV-Vis نشان می‌دهد که لایه‌ی روکش‌دار میتواند میزان رهاسازی را کنترل کند تا پتانسیل سازه‌ها را برای حمایت از مینرالیزاسیون بهبود بخشد. انتشار DEX بالاتر از GP بود و پس از ۹ روز به یک سرعت ثابت رسید. نتایج آزمایش MTT، مناسب بودن سطح Ti طراحی شده را برای بازسازی بافت استخوانی تایید می‌کند.

doi: 10.5829/ije.2019.32.10a.01